ACS Chemical Neuroscience

Research Article

pubs.acs.org/chemneuro

# Palonosetron–5-HT$_3$ Receptor Interactions As Shown by a Binding Protein Cocrystal Structure

Kerry L. Price,[†] Reidun K. Lillestol,[†] Chris Ulens,[‡] and Sarah C. R. Lummis*[,†]

[†]Department of Biochemistry, University of Cambridge, Tennis Court Road, Cambridge CB2 1QW, United Kingdom

[‡]The Laboratory of Structural Neurobiology, Department of Cellular and Molecular Medicine, KU Leuven, Herestraat 49, PB 601, B-3000 Leuven, Belgium

**ABSTRACT:** Palonosetron is a potent 5-HT$_3$ receptor antagonist and an effective therapeutic agent against emesis. Here we identify the molecular determinants of compound recognition in the receptor binding site by obtaining a high resolution structure of palonosetron bound to an engineered acetylcholine binding protein that mimics the 5-HT$_3$ receptor binding site, termed 5-HTBP, and by examining the potency of palonosetron in a range of 5-HT$_3$ receptors with mutated binding site residues. The structural data indicate that palonosetron forms a tight and effective wedge in the binding pocket, made possible by its rigid tricyclic ring structure and its interactions with binding site residues; it adopts a binding pose that is distinct from the related antiemetics granisetron and tropisetron. The functional data show many residues previously shown to interact with agonists and antagonists in the binding site are important for palonosetron binding, and indicate those of particular importance are W183 (a cation–$\pi$ interaction and a hydrogen bond) and Y153 (a hydrogen bond). This information, and the availability of the structure of palonosetron bound to 5-HTBP, should aid the development of novel and more efficacious drugs that act via 5-HT$_3$ receptors.

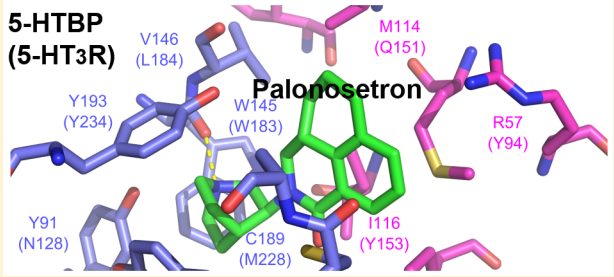


**KEYWORDS:** *Ligand-gated ion channel, Cys-loop receptor, serotonin receptor*

The 5-HT$_3$ receptors, like nicotinic acetylcholine (nACh), GABA$_{A/C}$, and glycine receptors, are members of the Cys-loop family of pentameric ligand-gated ion channels.[1] They play important roles in fast neurotransmission in the central and peripheral nervous systems. 5-HT$_3$ receptors are located primarily in the chemoreceptor trigger zone in the area postrema and in the gastrointestinal (GI) tract, where they have roles in regulating gut motility and the emesis reflex.[2]

Palonosetron (Aloxi; RS 25259-197) is a second generation 5-HT$_3$ receptor antagonist in clinical use which acts at both central and GI sites to reduce nausea and vomiting caused by chemotherapy, radiotherapy, or general anesthesia.[3] Compared to first-generation 5-HT$_3$ receptor antagonists, such as ondansetron and granisetron, palonosetron is more potent and has a longer half-life, making it a highly effective, long-lasting antiemetic.[4,5] It has some unusual properties that have not yet been fully explained, such as the prolonged inhibition of 5-HT$_3$ receptors by palonosetron; this may be due to an ability to cause receptor internalization, though an extremely slow dissociation rate could also explain this phenomenon.[6−10]

Palonosetron was discovered during the investigation of conformationally restricted analogues of granisetron.[11] Confirming previous findings, it was shown that the orientations of the amide carbonyl and the tertiary amine group relative to the aromatic nucleus were critical determinants of 5-HT$_3$ receptor affinity. The enhanced stability brought about by subsequent cyclization of the amide group with the aromatic structure is likely responsible for the increase in affinity compared to other 5-HT$_3$ receptor antagonists.

To probe the specific interactions of palonosetron in order to better understand its unusual properties, we have solved the structure of palonosetron bound to 5-HTBP, an acetylcholine binding protein (AChBP) from *Aplysia californica* (*Ac*) engineered to bind 5-HT and granisetron with high affinity.[12] This protein carries the mutations Y53W and Q55R and displays a 2.3-fold higher affinity for the 5-HT$_3$ receptor antagonist granisetron and a 5.8-fold higher affinity for 5-HT than the native AChBP. We have also mutated human 5-HT$_3$ receptor residues that contribute to the ligand-binding site (Figure 1), and characterized the potency of palonosetron in the resulting mutant receptors following expression in HEK293 cells.

## RESULTS AND DISCUSSION

**X-ray Crystal Structure of Palonosetron-Bound 5-HTBP.** A complete diffraction data set was collected from a crystal that diffracted to a resolution of 2.34 Å, which allowed determination of the 3-dimensional structure of 5-HTBP in complex with palonosetron (Table 1). The crystal belongs to the space group $P2_1$ and the crystallographic unit cell has the

**Received:** May 12, 2016
**Accepted:** September 8, 2016
**Published:** September 22, 2016

  

DOI: 10.1021/acschemneuro.6b00132
*ACS Chem. Neurosci.* 2016, 7, 1641−1646

```
                                                    Loop D
5HTBP     ------------------------------QANLMRLKSDLFN--RSPMYPGPTKDDPLT 28
Ac-AChBP  ------------------------------QANLMRLKSDLFN--RSPMYPGPTKDDPLT 28
h5HT3A    MLLWVQQALLALLLPTLLAQGEARRSRNTTRPALLRLSDYLLTNYRKGVRPVRDWRKPTT 60

                                                    Loop D
5HTBP     VTLGFTLQDIVKVDSSTNEVDLVYWERQRWKLNSLMWDPNEYGNITDFRTSAADIWTPDI 88
Ac-AChBP  VTLGFTLQDIVKVDSSTNEVDLVYYEQQRWKLNSLMWDPNEYGNITDFRTSAADIWTPDI 88
h5HT3A    VSIDVIVYAILNVDEKNQVLTTYIWYRQYWTDEFLQWNPEDFDNITKLSIPTDSIWVPDI 120

          Loop A          Loop E                                  Loop B
5HTBP     TAYSSTRPVQVLSPQIAVVTHDGSVMFIPAQRLSFMCDPTGVDSEEGVT-CAVKFGSWVY 147
Ac-AChBP  TAYSSTRPVQVLSPQIAVVTHDGSVMFIPAQRLSFMCDPTGVDSEEGVT-CAVKFGSWVY 147
h5HT3A    LINEFVDVGKSPNIPYVYIRHQGEVQNYKPLQVVTACSLDIYNFPFDVQNCSLTFTSWLH 180

                    Loop F                                  Loop C
5HTBP     SGFEID--L-KT-DTDQVDLSSYYASSKYEILSATQTRQVQHYSCCPEP-YIDVNLVVKFR 203
Ac-AChBP  SGFEID--L-KT-DTDQVDLSSYYASSKYEILSATQTRQVQHYSCCPEP-YIDVNLVVKFR 203
h5HT3A    TIQDINISLWRLPEKVKSDRSVFMNQGEWELL--GVLPYFREFSMESSNYYAEMKFYVVIR 239
```

**Figure 1.** Alignment of 5-HTBP, AChBP, and the extracellular domain of the human 5-HT3A receptor subunit showing the approximate location of the binding loops. The residues mutated in this study are highlighted in blue and magenta, and the residues that differ between 5-HTBP and AChBP are in yellow.

**Table 1**

| | 5HTBP+palonosetron |
|---|---|
| crystallographic statistics | |
| beamline | ID23-2 (ESRF) |
| wavelength (Å) | 0.873 |
| space group | $P2_1$ |
| $a,b,c$ (Å) | 72.21, 137.05, 131.25 |
| $\beta$ (deg) | 93.78 |
| resolution limits (Å) | 47.34−2.34 (2.47−2.34) |
| $R_{merge}$ (%) | 11.9 (84.5) |
| $R_{meas}$ (%) | 13.6 (95.6) |
| $\langle I/\sigma \rangle$ | 8.9 (1.6) |
| $CC_{1/2}$ (%) | 99.2 (59.8) |
| multiplicity | 4.5 (4.4) |
| completeness (%) | 98.8 (94.5) |
| total number of reflections | 476 641 (65 507) |
| number unique reflections | 106 052 (14 741) |
| refinement and model statistics | |
| $R_{work}$ (%) | 22.42 |
| $R_{free}$ (%) | 25.18 |
| rmsd bond distance (Å) | 0.0111 |
| rmsd bond angle (deg) | 1.691 |
| Ramachandran analysis | |
| outliers (%) | 0.0 |
| favored (%) | 99.06 |
| molprobity score | 0.96 (100th percentile) |

following dimensions: 72.21 Å ($a$), 137.05 Å ($b$), 131.25 Å ($c$), 90° ($\alpha$), 93.78° ($\beta$), and 90° ($\gamma$) and contains two pentamers per asymmetric unit.

**Palonosetron Interactions in 5-HTBP.** The data show that palonosetron could be built into the electron density at 7 out of 10 orthosteric binding sites. Each molecule is surrounded by predominantly aromatic and hydrophobic residues, including Y91, W145, Y186 and Y193 on the principal binding face, and W53, R55, V106, M114, and I116 on the complementary face (Figure 2A). The protonated quinuclidine N of palonosetron is within cation-$\pi$ interaction distance of W145 (W183 in the 5-$HT_3$ receptor), and there is a hydrogen bond between the protonated N of palonosetron and the backbone carbonyl of this residue. The near-planar tricyclic ring fits in a narrow pocket formed by the complementary face residues (mainly M114 and I116) and loop C of the principal face (Figure 2A). This location of palonosetron is similar to the

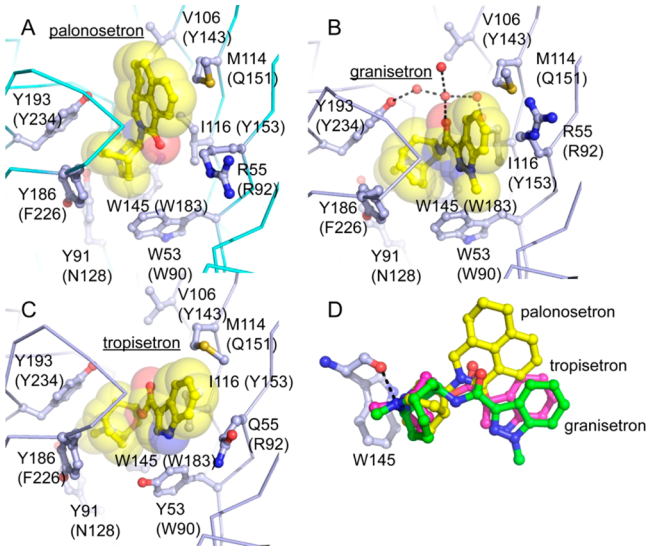


**Figure 2.** (A) 5-HTBP binding pocket showing the orientation of palonosetron and nearby residues. The protein backbone is shown in light blue ribbon presentation and side chains as ball and sticks. Palonosetron is shown as transparent spheres. Yellow is used for carbon, red for oxygen and blue for nitrogen. The corresponding 5-$HT_3$ receptor residues are in parentheses. (B, C) Similar presentations for the granisetron bound 5HTBP structure (pdb code 2YME) and tropisetron bound AChBP structure (pdb code 2WNC). (D) Relative binding poses of palonosetron (yellow), granisetron (green), and tropisetron (magenta) after superposition of the binding protein structures. The position relative to W145 is shown and the dashed line represents a hydrogen bond.

observed binding location of the well-studied 5-$HT_3$ receptor antagonist granisetron (Figure 2B), and also to the location predicted from experimental data for another antagonist ondansetron.[12,13] This location is also supported by computational studies, although one study docking palonosetron into the 5-$HT_3$ receptor suggested two binding sites, one in the orthosteric pocket and one below it; subsequent experimental data from mutant receptors, however, did not support this second binding site, and indicated that the effects of palonosetron are all manifest via the orthosteric binding pocket[10,14].

There are, however, some interesting differences between the palonosetron and granisetron structures. Interactions with


DOI: 10.1021/acschemneuro.6b00132
ACS Chem. Neurosci. 2016, 7, 1641−1646

water appear to be important for granisetron binding, where the structure suggested the oxygen of the amide bond may be involved in a hydrogen bonding network with five water molecules and Y193 (Y234 in the 5-HT$_3$ receptor),[12] but such a water network is not present in the palonosetron bound structure (Figure 2). Furthermore, rather than the structures overlapping, as might be expected from the common pharmacophore, they are rotated relative to each other (Figure 3). Thus, in the case of palonosetron the tricyclic ring system is

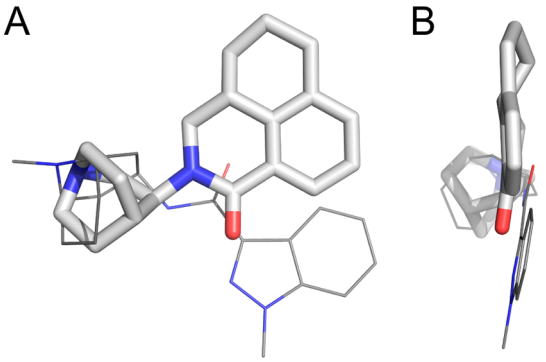


**Figure 3.** Superimposition of palonosetron (sticks) and granisetron (wireframe) as found in the crystal structures (palonosetron, this study; granisetron, 2YME) showing their different orientations in the binding site. (B) is a 90° rotation of the figure in (A).

tilted upward and centered relative to the complementary face residue M114 (Q151 in 5-HT$_3$) (Figure 2A). In contrast, granisetron is in a more downward position, in which the indazole moiety interacts with the complementary face residue R55 (R92 in 5-HT$_3$), forming a cation-$\pi$ interaction as previously described[12] (Figure 2B). Despite these differences in orientation between palonosetron and granisetron the positively charged nitrogen atoms are in nearly identical positions. A ligand binding pose very similar to granisetron was described in the cocrystal structure of Ac-AChBP with tropisetron (Figure 2C),[15] which is also used as an antiemetic and acts as a mixed antagonist for 5-HT$_3$ and a partial agonist for the $\alpha$7 nicotinic acetylcholine receptor.[16] It is possible that the different binding pose for palonosetron compared to granisetron and tropisetron (Figure 2D) could also explain some of the pharmacological differences between palonosetron and the other -setrons.

**Palonosetron Interactions at the Orthosteric Binding Site.** The affinities of 5-HT and granisetron at 5HTBP are considerably lower than when bound to 5-HT$_3$ receptors (e.g., ~100 fold difference in $K_i$ for granisetron), but nevertheless the critical elements of recognition in this protein are supported by many different studies.[12] We do not have a $K_i$ value for palonosetron, so to test if the orientation of palonosetron observed in the structure reflects binding to the 5-HT$_3$ receptor, substitutions of the human 5-HT$_3$ receptor residues equivalent to those within 5 Å of bound palonosetron were made, and inhibition of function by palonosetron was explored using membrane potential sensitive dye-loaded HEK293 cells in a Flexstation. Typical FlexStation responses are shown in Figure 4A, and an example concentration-inhibition curve from WT receptors is shown in Figure 4B. Palonosetron inhibition constants for WT and functional mutants are in Table 2. A number of mutants (L184A, F226A, M228C, Y234A, Y234S, W90A, Y141A, Y143A, Y143F, and Q151N) resulted in low or

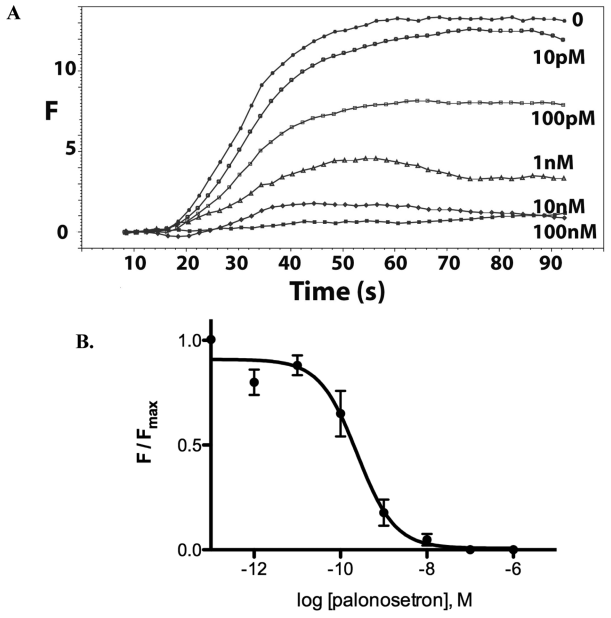


**Figure 4.** (A) Typical traces from HEK cells transfected with WT 5-HT$_3$ receptor cDNA, loaded with membrane potential dye, incubated with palonosetron at the concentrations shown, and stimulated at 20 s with 1 $\mu$M 5-HT. $F$ = arbitrary fluorescent units. (B) Typical concentration−inhibition curve for palonosetron constructed from FlexStation responses to WT 5-HT$_3$ receptors. Data = mean ± SEM, $n$ = 4.

no responses with 5-HT; some or all of these are likely to be important for palonosetron binding, as has been found for other 5-HT$_3$ receptor ligands.[17,18]

A plot of mutant receptor fold change in $p$EC$_{50}$ compared to WT/fold change in $p$K$_i$ compared to WT (Figure 5) is consistent with both ligands binding to the same site, although reveals some interesting differences in the importance of various residues. Those showing the most increased potency of palonosetron compared to 5-HT are N128A, N128Q and Y143S (>1.5 in Figure 5), consistent with their locations close to palonosetron. The data with N128A reflect both an increase in potency of palonosetron and a decrease in potency of 5-HT, the former possibly due to increased space in the binding site with a smaller residue, while the latter could be due to loss of a hydrogen bond which was revealed between the equivalent residue and 5-HT in the 5-HTBP structure.[12] Both these proposals are consistent with data from N128Q, which only show a decrease in potency of 5-HT. Data from Y143S reflects both an increase in potency for palonosetron and a decrease in potency for 5-HT, consistent with possible hydrophobic interactions of this residue with both 5-HT (unfavorable) and palonosetron (favorable).

The receptors showing the most decreased potency of palonosetron compared to 5-HT are those with W183A and Y153S substitutions. The data from W183A reveal a decrease in both 5-HT and palonosetron potency, but this is greater in the latter. W183 forms a cation−$\pi$ interaction with palonosetron both in the 5-HTBP structure and in the 5-HT$_3$ receptor. This is consistent with previous studies: W183 forms a cation-$\pi$ interaction with 5-HT, granisetron and ondansetron in the 5-HT$_3$ receptor, and the equivalent loop B aromatic residue also forms cation-$\pi$ interactions in some other Cys-loop receptors (e.g GABA$_C$ and nACh).[12,13,19] There is also a hydrogen bond with the backbone O in both 5-HT (2.7 Å distant) and


DOI: 10.1021/acschemneuro.6b00132
ACS Chem. Neurosci. 2016, 7, 1641−1646

**Table 2. Palonosetron Inhibition Constants for WT and Functional Mutants[a]**

| loop | residue | mutants | $pK_i \pm$ SEM (M) | $K_i$ (nM) | $n$ | 5-HT $pEC_{50}$ (M)[b] | $EC_{50}$ ($\mu$M) | $n$ |
|---|---|---|---|---|---|---|---|---|
| | | WT | 9.76 ± 0.11 | 0.17 | 8 | 6.51 ± 0.03 | 0.30 | 5 |
| A | N128 | N128A | 10.75 ± 0.17[c] | 0.018 | 6 | 5.47 ± 0.10[c] | 3.4 | 4 |
| | | N128Q | 9.60 ± 0.10 | 0.25 | 6 | 4.53 ± 0.02[c] | 29 | 4 |
| B | W183 | W183A | 5.13 ± 0.14[c] | 7400 | 8 | 3.88 ± 0.05[c] | 130 | 4 |
| | | W183Y | 7.51 ± 0.19[c] | 31 | 8 | 4.60 ± 0.03[c] | 25 | 5 |
| B | L184 | L184A | | | | NR | | 6 |
| | | L184I | 9.90 ± 0.20 | 0.13 | 5 | 5.56 ± 0.05[c] | 2.7 | 4 |
| C | F226 | F226A | | | | SR | | 6 |
| | | F226Y | 9.68 ± 0.22 | 0.21 | 4 | 5.72 ± 0.06[c] | 1.9 | 7 |
| C | M228 | M228A | 9.02 ± 0.27[c] | 0.96 | 6 | 5.03 ± 0.04[c] | 9.3 | 4 |
| | | M228C | | | | NR | | 6 |
| C | E229 | E229A | 10.31 ± 0.30 | 0.049 | 6 | 5.63 ± 0.04[c] | 2.3 | 6 |
| | | E229D | 10.00 ± 0.07 | 0.10 | 6 | 6.58 ± 0.05 | 0.26 | 3 |
| C | Y234 | Y234A | | | | NR | | 6 |
| | | Y234F | 10.35 ± 0.10 | 0.045 | 8 | 5.89 ± 0.03[c] | 1.3 | 4 |
| | | Y234S | | | | NR | | 6 |
| D | W90 | W90A | | | | NR | | 6 |
| | | W90Y | 9.58 ± 0.10 | 0.26 | 10 | 5.66 ± 0.05[c] | 2.2 | 5 |
| D | R92 | R92A | 9.29 ± 0.12 | 0.51 | 4 | 6.06 ± 0.04[c] | 0.87 | 4 |
| | | R92Q | 8.31 ± 0.09[c] | 4.9 | 8 | 4.82 ± 0.04[c] | 15 | 4 |
| D | Y94 | Y94A | 9.59 ± 0.05 | 0.26 | 8 | 7.24 ± 0.03[c] | 0.06 | 5 |
| | | Y94F | 9.00 ± 0.13[c] | 1.0 | 8 | 6.84 ± 0.04 | 0.15 | 6 |
| | | Y94S | 10.13 ± 0.17 | 0.074 | 6 | 7.03 ± 0.06[c] | 0.09 | 6 |
| | S114 | S114A | 9.26 ± 0.29 | 0.55 | 4 | 6.31 ± 0.05 | 0.49 | 7 |
| | | S114T | 9.96 ± 0.05 | 0.11 | 4 | 5.87 ± 0.27[c] | 1.4 | 3 |
| E | Y141 | Y141A | | | | NR | | 6 |
| | | Y141F | 10.10 ± 0.07 | 0.079 | 4 | 6.83 ± 0.03 | 0.15 | 3 |
| E | Y143 | Y143A | | | | NR | | 6 |
| | | Y143F | | | | SR | | 4 |
| | | Y143S | 10.51 ± 0.07 | 0.031 | 4 | 4.35 ± 0.03[c] | 45 | 3 |
| E | Q151 | Q151A | 10.21 ± 0.21 | 0.062 | 6 | 6.13 ± 0.06 | 0.74 | 4 |
| | | Q151N | 10.43 ± 0.14 | 0.042 | 3 | 6.34 ± 0.03 | 0.47 | 3 |
| E | Y153 | Y153A | 8.31 ± 0.08[c] | 4.9 | 3 | 4.73 ± 0.03[c] | 19 | 3 |
| | | Y153F | 8.40 ± 0.12[c] | 3.9 | 8 | 5.54 ± 0.03[c] | 2.9 | 3 |
| | | Y153S | 5.66 ± 0.09[c] | 2200 | 4 | 5.32 ± 0.06[c] | 4.8 | 3 |

[a]Data = mean ± SEM. [b]Data from ref 17. [c]Significantly different ($p < 0.05$) to WT 5-$HT_3$A receptors. NR = no response at 100 mM 5-HT; SR = responses too small to obtain parameters.

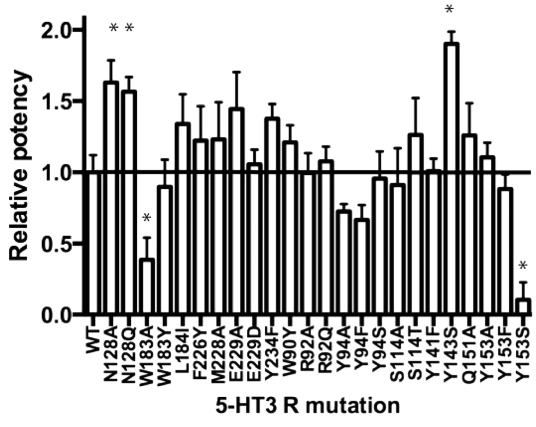


**Figure 5.** Plot of fold change in $pEC_{50}$ compared to WT/fold change in $pK_i$ compared to WT (relative potency) showing which mutations have stronger effects on 5-HT (<1) or palonosetron (>1). *Those discussed in the text.

palonosetron (2.5 Å distant). As hydrogen bonds show a fairly steep distance dependence, such that only a slight shift is needed to strengthen or weaken a hydrogen bond, while cation−$\pi$ interactions are much less sensitive to distance, we consider it likely that this hydrogen bond is more important for palonosetron than for 5-HT binding. We speculate that the lack of other hydrogen bonds between palonosetron and residues in the binding pocket makes this one more significant: 5-HT is predicted to have other hydrogen bonds but palonosetron is not.

The R92A mutation reveals an interesting difference between the effects of palonosetron and granisetron on the 5-$HT_3$ receptor. While no significant change in binding affinity was observed with palonosetron binding to R92A receptors, there was a reduction in binding affinity for granisetron.[18,20] This may be due to the cation−$\pi$ interaction R92 forms with the indazole portion of granisetron, which is apparent from both the 5-HTBP structural data and unnatural amino acid studies.[12] Such an interaction is not present in the palonosetron−5-HTBP structure as R92 is too far from palonosetron; the distance between the $\varepsilon$N of R55 (R92) and the center of the indazole ring of granisetron structure is 3.6 Å,[12] compared to an equivalent distance of 7.1 Å in the palonosetron structure; here the isoquinoline ring of palonosetron is higher up in the binding site than the indazole ring of granisetron (Figure 2A,B).


DOI: 10.1021/acschemneuro.6b00132
ACS Chem. Neurosci. 2016, 7, 1641−1646

The largest difference we observed in the functional data between palonosetron and 5-HT was for the Y153S mutant receptor (Figure 5) and is due to a much greater decrease of potency for palonosetron compared to 5-HT. This is not due to loss of the aromatic group, as Y153A mutant receptors have a similar palonosetron $K_i$ to those containing Y153F (both ∼10-fold greater than WT), consistent with data obtained with granisetron.[18,22,23] We therefore speculate that there is an interaction between the side chain of Ser and another residue, or with the ligand itself, which results in less energetically favorable antagonist binding. The equivalent residue is an isoleucine (I116) in 5-HTBP, so the role of this residue in the 5-$HT_3$ receptor is difficult to predict. However, other studies provide some guidance: Data from unnatural amino acid mutageneses indicate a hydrogen bond between the −OH of Y153 and 5-HT, consistent with a role of this residue in agonist binding,[17,21] and a similar interaction has been proposed with granisetron. It is therefore feasible that Y153 could form a hydrogen bond with the amide carbonyl of palonosetron. Indeed the precision of the distance and angles of this oxygen and the quinuclidine N with Y153 and W183, respectively could provide an explanation as to why these functional groups are crucial for the high affinity binding of palonosetron.[11]

Another residue that results in different effects for 5-HT and palonosetron when mutated is Y94 in loop D, as substitutions here to Ala or Ser enhance 5-HT $EC_{50}$s but have no effect on palonosetron $K_i$ values. We speculate that a bulky residue facing into the binding pocket may have a deleterious effect on agonist-induced conformational changes, which are not required for antagonists. We also observed mutations of N128 in Loop A and Y143S in loop E have distinct effects on 5-HT and palonosetron potencies at the functional level, consistent with different structures of the binding pocket in agonist and antagonist bound receptors.

In addition to the specific residue interactions, the structural data provide a further explanation for the efficacy of palonosetron, as its large surface area and planarity defined by the rigid tricyclic ring provides an opportunity for multiple aromatic and other hydrophobic interactions, which drive a highly effective wedge between loop C and the complementary face of the receptor (Figure 6).

## CONCLUSIONS

Our structural data showing the orientation of palonosetron in a 5-$HT_3$ receptor binding site mimic, combined with functional data in the 5-$HT_3$ receptor, provide an explanation for the high affinity and long-lived actions of this compound. These are likely due to specific interactions formed with binding site residues, and its location as a tight and effective wedge in the binding pocket, made possible by its tricyclic ring structure. This information, and the availability of the structure of palonosetron bound to 5-HTBP, should aid the development of novel even more potent and efficacious drugs that act via 5-$HT_3$ receptors.

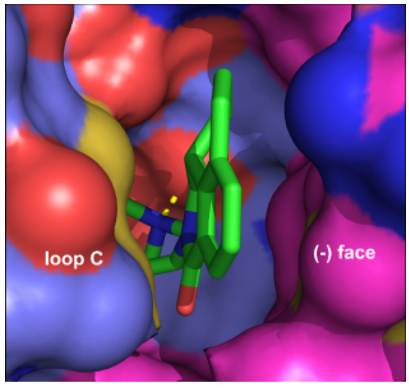


**Figure 6.** Image of palonosetron bound in 5-HTBP, revealing it forms a tight and effective wedge in the binding pocket.

## METHODS

**Protein Expression and Crystallization.** 5-HTBP (mutant D2) was expressed and purified as previously described.[12] Purified protein was concentrated to 6 mg/mL and a solution of palonosetron in water was added at a final concentration of 1 mM. Crystallizations screens were setup with a Mosquito crystallization robot (TTP Labtech). Crystals were obtained under a condition containing 200 mM sodium citrate, 100 mM bis tris propane pH 8.5, and 20% (w/v) PEG3350. Crystals were cryoprotected by adding glycerol in 5% (w/v) increments up to a concentration of 30% (w/v) and immersed in liquid nitrogen. X-ray diffraction data were collected at the ID23−2 beamline of the European Synchrotron Radiation Facility (ESRF, Grenoble). Reflections were integrated with XDS[24] and scaled in SCALA in the CCP4 suite.[25] The structure was solved using MOLREP[25] and the unliganded 5HTBP structure as a search model (pdb code 2yme). Structure building was done in Coot[26] and structure refinement was done in Phenix refine.[27] A final polishing refinement was done in PDB REDO.[28] Structure validation was done with Molprobity.[29] Figures were prepared with PyMOL (Schrödinger).

**Mutagenesis.** All mutant human 5-$HT_3$ receptors were created using QuikChange mutagenesis (Agilent).

**Cell Culture.** Human embryonic kidney (HEK) 293 cells were maintained on 90 mm tissue culture plates at 37 °C and 7% CO2 in a humidified atmosphere. They were cultured in Dulbecco's Modified Eagle's Medium/Nutrient Mix F12 (1:1) with GlutaMAX I media (Life Technologies, Paisley, UK) containing 10% HyClone fetal calf serum (GE Healthcare). For FlexStation studies, cells were transfected using polyethylenimine (PEI; Polysciences): 30 μL PEI (1 mg/mL), 5 μL cDNA (1 mg/mL; subcloned into pcDNA3.1), and 1 mL DMEM were incubated for 10 min at room temperature, added dropwise to a 70−90% confluent plate, and incubated for 2 days. Cells were then transferred to poly-L-lysine (Cultrex)-coated 96-well plates and allowed to adhere overnight before use.

**FlexStation Analysis.** The methods were as described previously.[17] In brief, fluorescent membrane potential dye (Membrane Potential Blue kit, Molecular Devices) was diluted in Flex buffer (10 mM HEPES, 115 mM NaCl, 1 mM KCl, 1 mM $CaCl_2$, 1 mM $MgCl_2$, and 10 mM glucose, pH 7.4) and added to each well of cells. The cells were incubated at 37 °C for 45 min with the dye and palonosetron (Alomone laboratories, Israel) and then fluorescence measured in a FlexStation (Molecular Devices) at 2 s intervals for 200 s. 5-HT (Sigma) was added to each well after 20 s. Data were normalized to the maximum $\Delta F$. 5-HT concentration−response data[17] and palonosetron concentration-inhibition data were analyzed using Prism (GraphPad Software Inc.) using the Leff and Dougall modification of the Cheng-Prusoff equation.[30]

## AUTHOR INFORMATION

### Author Contributions

Participated in research design: S.C.R.L., K.L.P., and C.U. Conducted experiments: R.K.L., K.L.P., C.U., and S.C.R.L. Performed data analysis: R.K.L., K.L.P., C.U., and S.C.R.L. Wrote or contributed to the writing of the manuscript: S.C.R.L., K.L.P., and C.U.

### Funding

Supported by a grant from the MRC (MR/L02/676) to S.C.R.L.



DOI: 10.1021/acschemneuro.6b00132
ACS Chem. Neurosci. 2016, 7, 1641−1646

### Notes

The authors declare no competing financial interest.

## ■ ACKNOWLEDGMENTS

We thank local contacts at beamline ID23-2 of the European Synchrotron Radiation Facility (ESRF, Grenoble) for assistance during data collection. Structure factors and atomic coordinates for 5HTBP-D2 in complex with palonosetron have been deposited with the Protein Data Bank under accession number 5LXB.

## ■ ABBREVIATIONS

5-HT, 5-hydroxytryptamine; nACh receptor, nicotinic acetylcholine; GABA, gamma-aminobutyric acid; HEK, human embryonic kidney; AChBP, acetylcholine binding protein

## ■ REFERENCES

(1) Lummis, S. C. (2012) 5-$HT_3$ receptors. *J. Biol. Chem. 287*, 40239−40245.
(2) Thompson, A. J., and Lummis, S. C. (2006) 5-$HT_3$ receptors. *Curr. Pharm. Des. 12*, 3615−3630.
(3) Navari, R. M. (2015) 5-HT receptors as important mediators of nausea and vomiting due to chemotherapy. *Biochim. Biophys. Acta, Biomembr. 1848*, 2738.
(4) Eglen, R. M., Lee, C. H., Smith, W. L., Johnson, L. G., Clark, R., Whiting, R. L., and Hegde, S. S. (1995) Pharmacological characterization of RS 25259−197, a novel and selective 5-$HT_3$ receptor antagonist, in vivo. *Br. J. Pharmacol. 114*, 860−866.
(5) Wong, E. H., Clark, R., Leung, E., Loury, D., Bonhaus, D. W., Jakeman, L., Parnes, H., Whiting, R. L., and Eglen, R. M. (1995) The interaction of RS 25259−197, a potent and selective antagonist, with 5-$HT_3$ receptors, in vitro. *Br. J. Pharmacol. 114*, 851−859.
(6) Hothersall, J. D., Moffat, C., and Connolly, C. N. (2013) Prolonged inhibition of 5-$HT_3$ receptors by palonosetron results from surface receptor inhibition rather than inducing receptor internalization. *Br. J. Pharmacol. 169*, 1252−1262.
(7) Rojas, C., Stathis, M., Thomas, A. G., Massuda, E. B., Alt, J., Zhang, J., Rubenstein, E., Sebastiani, S., Cantoreggi, S., Snyder, S. H., and Slusher, B. (2008) Palonosetron exhibits unique molecular interactions with the 5-$HT_3$ receptor. *Anesth. Analg. 107*, 469−478.
(8) Rojas, C., Thomas, A. G., Alt, J., Stathis, M., Zhang, J., Rubenstein, E. B., Sebastiani, S., Cantoreggi, S., and Slusher, B. S. (2010) Palonosetron triggers 5-$HT_3$ receptor internalization and causes prolonged inhibition of receptor function. *Eur. J. Pharmacol. 626*, 193−199.
(9) Lummis, S. C., and Thompson, A. J. (2013) Agonists and antagonists induce different palonosetron dissociation rates in 5-$HT_3$A and 5-$HT_3$AB receptors. *Neuropharmacology 73*, 241−246.
(10) Moura Barbosa, A. J., De Rienzo, F., Ramos, M. J., and Menziani, M. C. (2010) Computational analysis of ligand recognition sites of homo- and heteropentameric 5-$HT_3$ receptors. *Eur. J. Med. Chem. 45*, 4746−4760.
(11) Clark, R. D., Miller, A. B., Berger, J., Repke, D. B., Weinhardt, K. K., Kowalczyk, B. A., Eglen, R. M., Bonhaus, D. W., Lee, C. H., Michel, A. D., et al. (1993) 2-(Quinuclidin-3-yl)pyrido[4,3-b]indol-1-ones and isoquinolin-1-ones. Potent conformationally restricted 5-$HT_3$ receptor antagonists. *J. Med. Chem. 36*, 2645−2657.
(12) Kesters, D., Thompson, A. J., Brams, M., van Elk, R., Spurny, R., Geitmann, M., Villalgordo, J. M., Guskov, A., Danielson, U. H., Lummis, S. C., Smit, A. B., and Ulens, C. (2013) Structural basis of ligand recognition in 5-$HT_3$ receptors. *EMBO Rep. 14*, 49−56.
(13) Duffy, N. H., Lester, H. A., and Dougherty, D. A. (2012) Ondansetron and granisetron binding orientation in the 5-$HT_3$ receptor determined by unnatural amino acid mutagenesis. *ACS Chem. Biol. 7*, 1738−1745.
(14) Del Cadia, M., De Rienzo, F., Weston, D. A., Thompson, A. J., Menziani, M. C., and Lummis, S. C. (2013) Exploring a potential palonosetron allosteric binding site in the 5-$HT_3$ receptor. *Bioorg. Med. Chem. 21*, 7523−7528.
(15) Hibbs, R. E., Sulzenbacher, G., Shi, J., Talley, T. T., Conrod, S., Kem, W. R., Taylor, P., Marchot, P., and Bourne, Y. (2009) Structural determinants for interaction of partial agonists with acetylcholine binding protein and neuronal alpha7 nicotinic acetylcholine receptor. *EMBO J. 28*, 3040−3051.
(16) Macor, J. E., Gurley, D., Lanthorn, T., Loch, J., Mack, R. A., Mullen, G., Tran, O., Wright, N., and Gordon, J. C. (2001) The 5-$HT_3$ antagonist tropisetron (ICS 205−930) is a potent and selective alpha7 nicotinic receptor partial agonist. *Bioorg. Med. Chem. Lett. 11*, 319−321.
(17) Price, K. L., Lillestol, R. K., Ulens, C., and Lummis, S. C. (2015) Varenicline Interactions at the 5-$HT_3$ Receptor Ligand Binding Site are Revealed by 5-HTBP. *ACS Chem. Neurosci. 6*, 1151.
(18) Thompson, A. J., Price, K. L., Reeves, D. C., Chan, S. L., Chau, P. L., and Lummis, S. C. (2005) Locating an antagonist in the 5-$HT_3$ receptor binding site using modeling and radioligand binding. *J. Biol. Chem. 280*, 20476−20482.
(19) Beene, D. L., Brandt, G. S., Zhong, W., Zacharias, N. M., Lester, H. A., and Dougherty, D. A. (2002) Cation-pi Interactions in Ligand Recognition by Serotonergic (5-$HT_3$) and Nicotinic Acetylcholine Receptors: The Anomalous Binding Properties of Nicotine. *Biochemistry 41*, 10262−10269.
(20) Yan, D., Schulte, M. K., Bloom, K. E., and White, M. M. (1999) Structural features of the ligand-binding domain of the serotonin 5$HT_3$ receptor. *J. Biol. Chem. 274*, 5537−5541.
(21) Beene, D. L., Price, K. L., Lester, H. A., Dougherty, D. A., and Lummis, S. C. (2004) Tyrosine residues that control binding and gating in the 5-hydroxytryptamine3 receptor revealed by unnatural amino acid mutagenesis. *J. Neurosci. 24*, 9097−9104.
(22) Price, K. L., and Lummis, S. C. (2004) The role of tyrosine residues in the extracellular domain of the 5-hydroxytryptamine$_3$ receptor. *J. Biol. Chem. 279*, 23294−23301.
(23) Venkataraman, P., Venkatachalan, S. P., Joshi, P. R., Muthalagi, M., and Schulte, M. K. (2002) Identification of critical residues in loop E in the 5-$HT_3$ASR binding site. *BMC Biochem 3*, 15.
(24) Kabsch, W. (2010) XDS. *Acta Crystallogr., Sect. D: Biol. Crystallogr. 66*, 125.
(25) Winn, M. D., Ballard, C. C., Cowtan, K. D., Dodson, E. J., Emsley, P., Evans, P. R., Keegan, R. M., Krissinel, E. B., Leslie, A. G., McCoy, A., McNicholas, S. J., Murshudov, G. N., Pannu, N. S., Potterton, E. A., Powell, H. R., Read, R. J., Vagin, A., and Wilson, K. S. (2011) Overview of the CCP4 suite and current developments. *Acta Crystallogr., Sect. D: Biol. Crystallogr. 67*, 235−242.
(26) Emsley, P., Lohkamp, B., Scott, W. G., and Cowtan, K. (2010) Features and development of Coot. *Acta Crystallogr., Sect. D: Biol. Crystallogr. 66*, 486−501.
(27) Adams, P. D., Afonine, P. V., Bunkóczi, G., Chen, V. B., Davis, I. W., Echols, N., Headd, J. J., Hung, L. W., Kapral, G. J., Grosse-Kunstleve, R. W., McCoy, A. J., Moriarty, N. W., Oeffner, R., Read, R. J., Richardson, D. C., Richardson, J. S., Terwilliger, T. C., and Zwart, P. H. (2010) PHENIX: a comprehensive Python-based system for macromolecular structure solution. *Acta Crystallogr., Sect. D: Biol. Crystallogr. 66*, 213−221.
(28) Joosten, R. P., Long, F., Murshudov, G. N., and Perrakis, A. (2014) The PDB_REDO server for macromolecular structure model optimization. *IUCrJ 1*, 213−220.
(29) Chen, V. B., Arendall, W. B. r., Headd, J. J., Keedy, D. A., Immormino, R. M., Kapral, G. J., Murray, L. W., Richardson, J. S., and Richardson, D. C. (2010) MolProbity: all-atom structure validation for macromolecular crystallography. *Acta Crystallogr., Sect. D: Biol. Crystallogr. 66*, 12−21.
(30) Leff, P., and Dougall, I. G. (1993) Further concerns over Cheng-Prusoff analysis. *Trends Pharmacol. Sci. 14*, 110−112.


DOI: 10.1021/acschemneuro.6b00132
*ACS Chem. Neurosci.* 2016, 7, 1641−1646